

**Heterogeneous Chemistry of  $\text{HO}_2\text{NO}_2$  on Liquid Sulfuric Acid**

**Renyi Zhang, Ming-Taun Leu<sup>\*</sup>, and Leon F. Keyser**

Earth and Space Sciences Division

Jet Propulsion Laboratory

California Institute of Technology

Pasadena, California 91109

(Submitted to *J. Phys. Chem.*, June 8, 1995)

\* To whom correspondence should be addressed.

## Abstract

The interaction of  $\text{HO}_2\text{NO}_2$  (peroxynitric acid, PNA) vapor with liquid sulfuric acid surfaces was investigated for the acid contents ranging from 50 to 70 wt % and over a temperature range from 205 to 230 K, using a fast flow-reactor coupled to a chemical ionization mass spectrometer. PNA was observed to be physically taken up by liquid sulfuric acid, without undergoing irreversible aqueous phase reactions. The measured uptake coefficient was found to vary from about 0.2 on 55 wt %  $\text{H}_2\text{SO}_4$  to 0.06 on 70 wt % acid solution. From the time-dependent uptake, the quantity  $H\sqrt{D_l}$  (that is the product of the Henry's law coefficient and the square root of the liquid-phase diffusion coefficient) was obtained. The Henry's law volatility coefficient of PNA in liquid sulfuric acid was derived by estimating the liquid-phase diffusion coefficient based on a cubic cell model. In general, the solubility was found to increase with decreasing acid content and decreasing temperature. For a constant  $\text{H}_2\text{O}$  partial pressure of  $6.1 \times 10^{-4}$  Torr,  $H$  was determined to be  $2 \times 10^6 \text{ M atm}^{-1}$  at 205 K and  $1 \times 10^5 \text{ M atm}^{-1}$  at 222 K, as the acid content was varied from 55 to 70 wt %. The heterogeneous reaction between PNA and HCl on liquid sulfuric acid was also examined and was found to be very slow ( $\gamma < 10^{-4}$ ). The measured solubilities reveal that peroxynitric acid should exist predominantly in the gas phase under conditions characteristic of the mid- or lower latitude stratosphere. For winter time polar stratospheric conditions, however, incorporation of PNA into sulfate aerosols may lead to significant redistribution of PNA from the gas to condensed phases, thus affecting stratospheric  $\text{HO}_x$  and  $\text{NO}_x$  concentrations.

## Introduction

Heterogeneous reactions occurring on stratospheric sulfate aerosols have been known to enhance ozone destruction,<sup>1,2</sup> primarily by deactivating  $\text{NO}_x$  (i.e. the conversion of  $\text{NO}_x$  into  $\text{NO}_y$ ) and by converting relatively inactive reservoir chlorine species into reactive forms (i.e.  $\text{ClONO}_2$  and  $\text{HCl}$  into  $\text{Cl}_2$  and  $\text{HOCl}$ ) that are rapidly photolyzed to yield atomic chlorine, which catalytically destroys ozone. Under unperturbed stratospheric conditions, the sulfate aerosols are believed to consist of aqueous sulfuric acid of 40 to 80 wt %, with a mean diameter of about 0.1  $\mu\text{m}$  and a number density from 1 to 10  $\text{cm}^{-3}$ .<sup>3</sup> Although much effort has been made to study heterogeneous processes involving  $\text{N}_2\text{O}_5$ ,  $\text{ClONO}_2$ ,  $\text{HCl}$ , and  $\text{HOCl}$  on sulfate aerosols,<sup>1,2</sup> which promote the release of active chlorine and affect the  $\text{NO}_x$  budget, little is known on heterogeneous chemistry involving other nitrogen-containing acids and oxides on liquid sulfuric acid. For example, peroxynteric acid may have potential importance in aqueous atmospheric chemistry in at least two ways: incorporation of PNA into sulfate aerosols may alter the aerosol composition and repartition PNA from the gas to condensed phases (thus affecting the  $\text{HO}_x$  and  $\text{NO}_x$  budgets);  $\text{HO}_2\text{NO}_2$  may also engage in heterogeneous reactions, such as that with  $\text{HCl}$  to form  $\text{HOCl}$ , or decomposition to produce  $\text{HONO}$ .

In the stratosphere  $\text{HO}_2\text{NO}_2$  (PNA) is present at concentrations of a few tenths of part per billion by volume (ppbv) and is formed mainly by the reaction of  $\text{HO}_2$  with  $\text{NO}_2$ ,<sup>4,5</sup>



The fate of gaseous PNA is governed by unimolecular decomposition as well as photodissociation and bimolecular reaction with OH. Under stratospheric conditions, PNA is recognized to be photochemically stable, with a lifetime about a few days.<sup>6,7</sup> Photolysis of PNA at wavelengths greater than 290 nm yields primarily  $\text{HO}_2$  and  $\text{NO}_2$ , along with minor HO and  $\text{NO}_3$ .<sup>8</sup> The bimolecular reaction of PNA with OH is very efficient, with a rate coefficient of  $4.6 \times 10^{-12} \text{ cm}^3 \text{ s}^{-1}$ ;<sup>1</sup> this reaction channel provides an important sink for OH radicals in the stratosphere. Other likely homogeneous reaction pathways include the reactions of PNA with O, H, and HCl, although these reactions are several orders of magnitude slower than that between PNA and OH.<sup>1</sup>

In contrast, the role of PNA in heterogeneous atmospheric chemistry is less certain. In aqueous solutions  $\text{HO}_2\text{NO}_2$  undergoes unimolecular decomposition producing  $\text{HONO}$  and  $\text{O}_2$ ,<sup>9,10</sup>



The decomposition rate ( $\sim 7 \times 10^{-4} \text{ s}^{-1}$ ) measured in these studies, however, suggests this reaction may be too slow to be of atmospheric importance, unless the Henry's law volatility for PNA is extremely large. In another recent study it has been postulated that heterogeneous decomposition of PNA may be responsible for significant production of nitrous acid (HONO) observed in an environmental chamber experiment.<sup>11</sup> The same reaction mechanism has also been invoked to explain the observed anomalous OH and HO<sub>2</sub> concentrations shortly after sunrise in stratospheric measurements:<sup>12,13</sup> this process occurring on sulfate aerosols may increase the diurnally averaged HO<sub>x</sub> by reducing an important HO<sub>x</sub> sink (i.e. PNA reaction with OH) and by redistributing HO<sub>x</sub> at larger solar zenith angles. Recently, Li et al.<sup>14</sup> have investigated PNA uptake on water ice. These authors reported a sticking coefficient of 0.15 for PNA on ice at about 200 K, with no reaction products. The uptake coefficient of PNA on 96 wt % sulfuric acid was also investigated by Baldwin and Golden at room temperature,<sup>15</sup> yielding a value of  $2.7 \times 10^{-5}$ . Clearly, more laboratory studies are needed in order to elucidate the interaction of PNA with sulfate aerosols in the stratosphere.

In this paper we present laboratory measurements of critical parameters needed to quantify the interaction of PNA vapor with liquid sulfuric acid. These include the uptake coefficient and volatility of PNA in liquid H<sub>2</sub>SO<sub>4</sub>. The product of the Henry's law coefficient and the square root of the liquid-phase diffusion coefficient,  $H\sqrt{D_l}$ , for PNA uptake was measured. The Henry's law volatility coefficient was then deduced by estimating the liquid-phase diffusion coefficient based on a cubic cell model. Potential heterogeneous reaction involving HO<sub>2</sub>NO<sub>2</sub> with HCl on liquid sulfuric acid was also examined. Finally, Stratospheric implications of the present data are discussed. In a separate publication we report laboratory experiments of heterogeneous chemistry of HONO and NO<sub>2</sub> on liquid sulfuric acid.<sup>16</sup>

## Theoretical Approach

In general, gas-phase uptake by a planar liquid surface can be due to time-dependent physical adsorption or irreversible chemical reaction, which can be treated as a one-dimension diffusion problem,

$$\frac{\partial C}{\partial t} = D_l \frac{\partial^2 C}{\partial x^2} - R \quad (3)$$

where  $C$  represents the concentration in the liquid,  $x$  is the distance, and  $R$  is the rate of liquid phase reaction. For the case where there is no chemical loss in the liquid (i.e.  $R = 0$ ), the time-dependent solution for eq. 3 can be written as,<sup>17-20</sup>

$$\frac{1}{\gamma_{obs}(t)} = \frac{1}{\alpha} + \frac{\omega}{4RTH(D_l)} t^{\frac{1}{2}} \quad (4)$$

where  $\alpha$  is the mass accommodation coefficient and  $\omega$  is the mean thermal speed of the molecule. Hence, equation 4 relates the measured uptake coefficient ( $\gamma_{obs}$ ) to the product of the Henry's law volatility coefficient and the square root of the liquid-phase diffusion coefficient ( $H/D_l$ ). The uptake coefficient can be calculated from

$$\gamma_{obs}(t) = \frac{2rk}{\omega + rk} \quad (5)$$

where  $r$  is the radius of the flow reactor. The first-order rate coefficient ( $k$ ) is related to the fractional change ( $\Delta n/n$ ) in the gas-phase concentration of the adsorbed/reactive molecule before and after exposure to liquid sulfuric acid by

$$k = \frac{2F_g}{rA} \frac{\Delta n}{n} \quad (6)$$

where  $F_g$  is the carrier gas volume rate of flow ( $\text{cm}^3 \text{S}^{-1}$ ) and  $A$  is the surface area of exposed liquid. When the uptake rate became gas-phase diffusion limited, the first-order rate coefficient was corrected for gas-phase diffusion restrictions according to the method suggested by Brown.<sup>21</sup> The gas-phase diffusion coefficient for PNA in He was estimated to be  $PD_g = 240 \text{ Torr cm}^2 \text{S}^{-1}$  at 220 K, with a temperature dependence of  $T^{1.5}$ .<sup>22</sup> From the time evolution of the signal for the adsorbed molecule, the quantity  $H/D_l$  can be extracted from the slope of a plot of  $1/\gamma_{obs}(t)$  versus  $t^{1/2}$ , according to eq.4.

An alternative approach for obtaining  $H/D_l$ , derived directly from the Henry's law (i.e. from the ratio of surface to gas concentrations of the species), has been suggested by Hanson and Ravishankara,<sup>20</sup>

$$H\sqrt{D_l} = \frac{2I(t)F_s}{S_oART\sqrt{\pi t}} \quad (7)$$

where  $S_o$  is the signal when no uptake takes place and  $I(t) = S_o t - \int S(t)dt$ . Using both methods, we obtained  $H\sqrt{D_l}$  that agreed within 25 %.

To estimate the liquid-phase diffusion coefficient, we adopted a cubic cell model, which was initially developed for self-diffusion in liquids,<sup>23,24</sup>

$$D_l = \frac{RT\rho\lambda^2}{6\eta M} \quad (8)$$

and

$$\lambda = \frac{1}{2} \left( d + \left[ \frac{xM_{SO_4} + (1-x)M_{H_2O}}{\rho} \right]^{\frac{1}{3}} \right) \quad (9)$$

where  $\rho$  is the density of liquid  $H_2SO_4$ ,  $M$  is the molecular weight of  $HO_2NO_2$ , and  $x$  is the  $H_2SO_4$  mole fraction. Assuming that there is no liquid-phase dissociation, we estimated an effective molecular dimension ( $d$ ) of  $\sim 4 \text{ \AA}$  for PNA diffusing in liquid sulfuric acid, when calculating the parameter for the effective cell dimension ( $\lambda$ ). The viscosity coefficient ( $\eta$ ) of sulfuric acid, used in eq. 8, was taken from Luo et al.,<sup>24</sup> which incorporated the viscosity measurements for 60 wt %  $H_2SO_4$  by Williams and Golden.<sup>25</sup> Table 1 lists some calculated values of the diffusion coefficient for PNA in sulfuric acid.

## Experimental Method

Uptake measurements were conducted in a fast flow reactor in conjunction with chemical ionization mass spectrometry (CIMS) detection. Detailed descriptions of the experimental apparatus and procedures have been given elsewhere,<sup>26-28</sup> and only a brief overview is presented here along with features pertinent to this work.

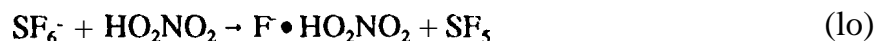
The flow reactor of inner diameter 2.8 cm was horizontal] y-mounted and temperature regulated. Liquid  $H_2SO_4$  films were prepared by totally covering the inside wall of the flow tube with sulfuric acid solutions, At low temperatures ( $< 220 \text{ K}$ ) the solutions were sufficiently

viscous to produce an essentially static film which lasted over the time scale of the experiments. The thickness of the films was estimated to be about 0.1 mm based on the amount of acid solution used and the geometric area covered. Composition of the liquid  $\text{H}_2\text{SO}_4$  film was governed by temperature and  $\text{H}_2\text{O}$  partial pressure in the flow tube: once exposed to  $\text{H}_2\text{O}$  vapor, the sulfuric acid film took up  $\text{H}_2\text{O}$  and became more dilute until equilibrium was reached.  $\text{H}_2\text{O}$  vapor was admitted to the flow tube with the main He carrier gas. The partial pressure of  $\text{H}_2\text{O}$  was estimated by passing a known flow of He carrier gas through a  $\text{H}_2\text{O}$  reservoir at room temperature. It was controlled by diluting the humidified He flow (assuming 100% RH) with a dry He flow. In addition, we measured  $\text{ClONO}_2$  hydrolysis on the liquid  $\text{H}_2\text{SO}_4/\text{H}_2\text{O}$  film and obtained its composition, on the basis of our earlier data of reaction probabilities for this binary system,<sup>26</sup> to validate the above method. The estimated uncertainty in determining the  $\text{H}_2\text{O}$  partial pressure was about  $\pm 25\%$ . To deduce the  $\text{H}_2\text{SO}_4$  content of the liquid film, we used the temperature and  $\text{H}_2\text{O}$  partial pressure to convert the  $\text{H}_2\text{SO}_4$  wt %, according to the vapor pressure data of Zeleznik<sup>29</sup> and Zhang et al.<sup>30</sup> The error limit in estimating the  $\text{H}_2\text{SO}_4$  content of the films was about  $\pm 3$  wt %, considering uncertainties associated with the temperature and water vapor pressure.

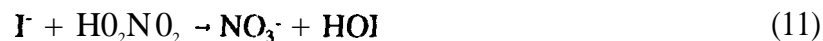
PNA was synthesized by slowly adding -1 g  $\text{NO}_2\text{BF}_4$  (Aldrich) to ~ 5 ml 93 wt %  $\text{H}_2\text{O}_2$  which was chilled (at 273 K) and vigorously stirred, according to the method described by Kenley et al.<sup>9</sup> The solution containing PNA was then transferred to a bubbler maintained at 273 K. The purity of PNA samples was checked both by infrared spectroscopy and mass spectrometry, with  $\text{NO}_2$ ,  $\text{HNO}_3$ ,  $\text{H}_2\text{O}_2$ , and  $\text{H}_2\text{O}$  being the major impurities. Generally, the amounts of  $\text{HNO}_3$  and  $\text{NO}_2$  in the PNA sample were reduced significantly after bubbling the solution for more than 10 min. A jacketed Pyrex injector (1.0-cm o.d.), kept warm by circulating a room temperature solution of ethylene glycol in water, was used to deliver PNA to the flow reactor. Gaseous PNA was added to the flow tube along with a small He flow (0.1-10.0  $\text{cm}^3 \text{min}^{-1}$  at STP) and further diluted in the main He flow (310  $\text{cm}^3 \text{min}^{-1}$  at STP) before contacting the liquid acid surface. To reduce the  $\text{H}_2\text{O}_2$  and  $\text{H}_2\text{O}$  impurities, the PNA flow was circulated through a cold trap at temperatures between 230 and 240 K, prior to entering the flow tube. A 3-way switching valve was designed to quickly change the PNA flow either downstream or upstream (i.e. to expose or bypass PNA gas to sulfuric acid), with a delay time less than 50 milliseconds.

Typically, the flow tube was operated at a pressure of about 0.40 Torr, with an average flow velocity ranging from 1700 to 2000 cm s<sup>-1</sup>.

In most experiments, HO<sub>2</sub>NO<sub>2</sub> was detected in the CIMS as F • HO<sub>2</sub>NO<sub>2</sub>, produced by a fluoride ion transfer with SF<sub>6</sub><sup>-</sup>,



A typical mass spectrum of SF<sub>6</sub><sup>-</sup> reaction with the effluent from the PNA bubbler is displayed in Figure 1, showing the characteristic HO<sub>2</sub>NO<sub>2</sub> peak (F • HO<sub>2</sub>NO<sub>2</sub>, *m/e* = 98) along with the impurity peaks due to NO<sub>2</sub> (NO<sub>2</sub><sup>-</sup>, *m/e* = 46) and HNO<sub>3</sub> (F • HNO<sub>3</sub>, *m/e* = 82). We are not aware of any measurements of the rate coefficient for reaction 10. The PNA concentration in the neutral flow reactor was estimated by assuming the same rate coefficient for reaction 10 as that for HNO<sub>3</sub> reaction with SF<sub>6</sub><sup>-</sup> (- 2x10<sup>-9</sup> molecule cm<sup>3</sup> s<sup>-1</sup>)<sup>31</sup> and by comparing the relative signal intensities between the two species under identical conditions. This method requires accurate knowledge of the gas-phase partial pressure of HNO<sub>3</sub>. The CIMS was calibrated for HNO<sub>3</sub> by measuring the flow rate of a known mixture of HNO<sub>3</sub> in He; the calibration procedure was described in detail in our previous works.<sup>26,27</sup> Alternatively, the I<sup>-</sup> ions, initiated by electron attachment to CF<sub>3</sub>I, were used to detect HO<sub>2</sub>NO<sub>2</sub> corresponding to NO<sub>3</sub><sup>-</sup> (*m/e* = 62), as illustrated in Figure 2,



Reaction 11 also permits selectively probe PNA in the presence of HNO<sub>3</sub>, because the reaction of I<sup>-</sup> with HNO<sub>3</sub> is known to be rather inefficient.<sup>31</sup> Hence, HNO<sub>3</sub> impurity present in the PNA sample is unlikely to interfere with this detection scheme. Indeed, using both SF<sub>6</sub><sup>-</sup> and I<sup>-</sup> as the reactant ions yielded no noticeable difference in the measurements of PNA uptake studies. To our knowledge, the rate coefficient for reaction 11 is unknown. Note that in the present uptake study accurate determination of the reactant concentration is not required, although lower reactant concentrations were essential to minimize the occurrence of secondary reactions of potential product ions,

Ions were mass selected by a differentially pumped mass spectrometer and detected with a channel electron multiplier operated in an analogue mode. The CIMS detector was linear over the range of PNA concentrations used, since the concentration of reactant ion was not affected



by the small concentrations of the neutral reactant, Detection sensitivity for  $\text{HO}_2\text{NO}_2$  in the CIMS was estimated to be  $\sim 10^8$  molecules  $\text{cm}^{-3}$  with a S/N ratio of 2.

## Results and Discussion

### *PNA Uptake Measurements*

The uptake of PNA by liquid sulfuric acid was studied by first establishing a steady-state PNA flow, which bypassed the liquid film. The direction of the PNA flow was then quickly changed from downstream to upstream via the 3-way switching valve, exposing a 3-10 cm length of the film to PNA while monitoring the PNA signal using the CIMS. Uptake from the gas phase was determined from the decline and recovery in the PNA signal. Figure 3 shows temporal profiles of PNA as it was exposed and not exposed to a 3.9 cm length of liquid sulfuric acid film at 207.9, 218.9, and 226.8 K, respectively. The liquid film was initially allowed to equilibrate with  $\text{H}_2\text{O}$  vapor at a partial pressure of  $6.9 \times 10^{-4}$  Torr and at 207.9 K; the acid content of the film was estimated to be  $\sim 58.3$  wt %. Temperature of the flow tube was quickly raised and then held steady at a higher value to carry out the next measurement. We assumed that compositional change in the liquid film was negligible during the whole process (typically less than 20 rein). The experimental conditions corresponding to these measurements were  $P_{\text{He}} = 0.40$  Torr,  $V \approx 1900$   $\text{cm}^3/\text{s}$ , and  $P_{\text{PNA}} \approx 5 \times 10^{-7}$  Torr.

Figure 3 shows that the PNA concentration in the gas phase fell instantly upon exposed to liquid  $\text{H}_2\text{SO}_4$  and later returned to its original value as the film was saturated. Switching the PNA flow downstream resulted in an opposite peak due to PNA resorption. The shapes of adsorption and resorption processes were identical, suggesting that PNA was physically taken up by liquid sulfuric acid without undergoing irreversible aqueous phase reactions. This held true over the entire  $\text{H}_2\text{SO}_4$  content and temperature ranges investigated, i.e., over  $\text{H}_2\text{SO}_4$  contents of 50-70 wt % and temperatures of 205-230 K. As can be seen from Figure 3, the uptake of PNA increased as the temperature decreased for a fixed sulfuric acid content. This occurred because solubility of PNA increased with decreasing temperature, as discussed in detail below. Under no circumstances did we observe any gaseous products by the CIMS associated with PNA uptake

in sulfuric acid. In particular, we found no evidence for the occurrence of reaction 2 on liquid sulfuric acid.

To test whether reaction 2 proceeds slowly on liquid sulfuric acid, as being the case suggested in aqueous  $\text{O}_2$ -saturated nitrate solutions,<sup>10</sup> we exposed PNA continuously to sulfuric acid over a time period of more than three hours and then identified the constituents in the liquid phase, using the temperature programmed desorption method. Two measurements were carried out for liquid films with contents of 50 and 70 wt % and at temperatures of 201 and 222 K, respectively. No reaction products other than PNA were observed in these experiments. (HONO can be detected using  $\text{SF}_6^-$  corresponding to  $\text{F} \bullet \text{HONO}$  at  $m/e = 66$ .)<sup>16</sup> Also, the  $\text{NO}_2$  impurity present in the PNA sample was too small to produce any appreciable amount of nitrous acid by the reaction of  $\text{NO}_2$  with  $\text{H}_2\text{O}$ . This reaction, however, may occur if very high  $\text{NO}_2$  concentrations are present,<sup>16</sup> and it may explain the observation of HONO product in the environmental chamber experiment reported by Zhu et al.,<sup>11</sup> likely with  $\text{NO}_2$  derived from thermal decomposition of PNA. As reported in a separate publication by us,<sup>16</sup> HONO undergoes complex aqueous phase reactions in liquid sulfuric acid, depending on the acidity.

#### *Uptake Coefficients.*

The initial decays of PNA signal upon exposure to liquid sulfuric acid, as those displayed in Figure 3, were used to determine the uptake coefficients. The measured uptake coefficient reflects the kinetics of the uptake, equilibrium solubility limitation, and gas-phase diffusion limitation. The values obtained after corrections for the gas-phase diffusion are depicted in Figure 4 as a function  $\text{H}_2\text{SO}_4$  wt %. The experiments were performed by maintaining a constant  $\text{H}_2\text{O}$  vapor pressure of  $6.1 \times 10^{-4}$  Torr and by varying the temperature from 205 to 222 K. The resulting acid content ranged from 56 to 70 wt %. A PNA partial pressure of  $5 \times 10^{-7}$  Torr was used in these experiments. Each point in the figure is an average over at least two measurements, with the error bars indicating experimental precision (1  $\sigma$ ). Systematic error in the uptake coefficient measurements was estimated to be about 15 %.

Figure 4 shows that the PNA uptake coefficient decreases as the acid content increases:  $\gamma$  ranges from about 0.2 to 0.06, as the acid content is varied from 56 to 70 wt %  $\text{H}_2\text{SO}_4$ . The

observed decrease is indicative of changes in either PNA solubility in the bulk  $\text{H}_2\text{SO}_4$  solution or accommodation probability at the surface, as a function of  $\text{H}_2\text{SO}_4$  composition. With an initial delay time of  $\sim 0.1$  second (i.e. the initial exposure time) for experiments used to produce Figure 4,  $D_1$  estimated from the cubic cell model, and the Henry's coefficient determined in the next section (i.e.  $2 \times 10^6$  to  $1 \times 10^5 \text{ M atm}^{-1}$  from 205 to 222 K), eq. 4 predicts that the measured uptake coefficient should be close to the value of accommodation ion coefficient ( $\alpha$ ) for  $\text{H}_2\text{SO}_4$  less than 60 wt %, For solutions more than 60 wt %, the measured uptake coefficients should be smaller than  $\alpha$ , because the uptake was limited by re-evaporation of dissolved PNA due to saturation of the liquid. Similarly, we believe that the uptake coefficient for 96 wt %  $\text{H}_2\text{SO}_4$  at room temperature ( $\gamma = 2.7 \times 10^{-5}$ ), reported by Baldwin and Golden,<sup>15</sup> is likely volatility limited.

#### Determination of $H\sqrt{D_1}$ and $H$

Uptake of PNA into sulfuric acid may take several steps, including solvation, dissociation, and ionic reactions with the constituents in the liquid,<sup>10</sup>



The acid equilibrium constant for PNA in aqueous nitrite solutions was determined to be  $1.4 \times 10^{-6}$  at room temperature,<sup>10</sup> indicating that PNA is a relatively weak acid. Under stratospheric conditions, reaction 14, along with reaction 2 and unimolecular decomposition of PNA into  $\text{HO}_2$  and  $\text{NO}_2$ , can be ignored in sulfuric acid, as concluded in the proceeding section. An effective Henry's law constant that encompasses the totality of the dissolved species is defined as,<sup>18</sup>

$$\text{H}' \leftarrow H \{1 + k_1 \gamma / [\text{H}']\} \quad (15)$$

$$[\text{HO}_2\text{NO}_2(\text{total})] = [\text{HO}_2\text{NO}_2(\text{aq})] + [\text{O}_2\text{NO}_2^-] = P_{\text{PNA}} H' \quad (16)$$

where  $H$  is the physical Henry's law constant (i.e. the equilibrium constant for reaction 12). Since eq. 7 is derived by determining the total number of molecules lost from the gas to liquid phases over an integrated time and using eq. 16,<sup>20</sup> the obtained volatility should be a measure of the effective Henry's law constant.

Measured values of  $H^*\sqrt{D_l}$  for PNA on sulfuric acid of various contents are shown against the reciprocal of temperature in Figure 5. The measurements were carried out by first establishing an equilibrium sulfuric acid film with a given  $H_2O$  partial pressure and temperature. The temperature of the substrate was then successively raised while the uptake data were taken. Due to the relatively short time scale during the whole process (i.e. less than 20 rein), we assumed that the acid content remained unchanged (i.e., evaporation of water from the sulfuric acid film would not cause an appreciable change in the acid content on a relatively short time scale at temperatures below 230 K). Examples of the uptake and desorption data have been given in Figure 3. Figure 5 shows that the quantity  $H^*\sqrt{D_l}$  increases both as the temperature is lowered and as the solution becomes more dilute. This is expected since physical solubility in general increases with decreasing temperature and decreasing acid content. Additionally, it is also plausible that the extent of PNA dissociation may enhance slightly at lower temperatures and in dilute sulfuric acid, as being the case with  $HNO_3$  in sulfuric acid,<sup>32</sup> thus leading to larger values for the effective Henry's law constants. Measurements of the quantity  $H^*\sqrt{D_l}$  for PNA on various sulfuric acid solutions are also listed in Table 2.

In a separate set of experiments, PNA uptake was studied by maintaining a constant  $H_2O$  partial pressure and by varying temperature and allowing water vapor to equilibrate with the liquid. This is a process that resembles the compositional change of sulfate aerosols during a cooling or warming event in the stratosphere. The results are presented in Figure 6 which plots  $H^*\sqrt{D_l}$  as a function of temperature. Each point in the figure is an average over two more measurements. It is evident in Figure 6 that the measured  $H^*\sqrt{D_l}$  increases with decreasing temperature. As discussed above, this profound temperature dependence is caused both by changing temperature and by changing  $H_2SO_4$  content, when  $P_{H_2O}$  is held constant. The diffusion coefficient, calculated from the cubic cell model, also changes with temperature and with  $H_2SO_4$  content: it decreases with decreasing temperature and increasing acid content. Thus the influences of temperature and acid content on the diffusion coefficient cancel out, resulting in little variation of  $D_l$  with temperature at a fixed  $P_{H_2O}$ . This implies that the observed increase in the quantity  $H^*\sqrt{D_l}$  in Figure 6 is attributable merely to the increase in the effective Henry's constant (also see Figure 8). The data shown in Figure 6 are tabulated in Table 3.

Effective Henry's constants were derived by estimating the liquid-phase diffusion coefficient for PNA in sulfuric acid.  $H^*$  corresponding to data in Figure 5 are given in Figure 7. For  $\text{H}_2\text{SO}_4$  content more than 70 wt %, the diffusion coefficient calculated from the cubic cell model appears to be unreliable, because the resultant  $H^*$  becomes decreasing with decreasing acid content at a given temperature, an unrealistic situation. This may be partially attributed to the lack of measurements for the viscosity coefficient in concentrated sulfuric acid ( $\geq 70$  wt %) at low temperatures. The slopes of the lines in the figure represent the difference between enthalpies of PNA in solution and in the gas-phase, which are correlated with the enthalpy changes of reactions 12 and 13. Figure 7 shows that the volatility constants for all the solutions have similar temperature dependencies, indicating a constant activity coefficient for each solution over the temperature range and, thus, little change in PNA dissociation over the composition range. It should be pointed out that available information on liquid-phase diffusion in sulfuric acid is very limited. Hence, the estimate of  $D$ , using the cubic cell model may contain considerable uncertainty.

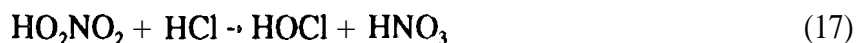
In Figure 8 are plotted  $H^*$  against stratospheric temperature for a water partial pressure of  $6.1 \times 10^{-4}$  Torr, based on data presented in Figure 6. A least squares fit through the data results in the expression of  $\log H^* = 149.01 - 1.274 \times T + 0.00282 \times T^2$ . Figure 8 shows that the effective Henry's law constant increases by an order of magnitude from 222 to 205 K. This increase is qualitatively similar to that of the quantity  $H^* \sqrt{D_i}$  shown in Figure 6, due to the fact that  $D_i$  changes relatively little with temperature, as mentioned in the above paragraph. Note that a lower stratospheric water partial pressure will lead to smaller  $H^*$  for a given temperature, since the sulfate aerosol composition is controlled both by temperature and by water partial pressure in the stratosphere.

The uptake measurements reported here were restricted to temperatures above 205 K. Below this temperature, the time scale to saturate the liquid film became so long that the PNA source became unstable. Also, at low temperatures and in dilute sulfuric acid, the Henry's law may not be a valid description of the volatility behavior, because of the departure from ideality or increasing activity coefficient.<sup>33</sup> Volubility of PNA in liquid sulfuric acid, as determined in the present study, is fairly large: under identical conditions (i.e. the same  $\text{H}_2\text{SO}_4$  content and

temperature) the effective Henry's law constant for PNA is smaller than that of  $\text{HNO}_3$ ,<sup>33</sup> but larger than that of  $\text{HCl}$ .<sup>20,24,25,33</sup> Hence, it would be worthwhile to examine some potential heterogeneous reactions involving PNA on sulfuric acid,

#### *Reaction of $\text{HO}_2\text{NO}_2$ with $\text{HCl}$*

The gas-phase reaction between  $\text{HO}_2\text{NO}_2$  and  $\text{HCl}$  has been found to be very slow, with a rate constant of less than  $9 \times 10^{-22} \text{ cm}^3 \text{ s}^{-1}$ ,<sup>34</sup>



This reaction, if proceeding in bulk sulfuric acid solutions, will likely produce gaseous  $\text{Cl}_2$  or  $\text{HOCl}$ , dependent on the relative concentrations between  $\text{HCl}$  and PNA.<sup>26,35</sup> This occurs because the secondary reaction between the product  $\text{HOCl}$  with  $\text{HCl}$  will take place in the solution to form  $\text{Cl}_2$ . The experiments were carried out by first allowing the  $\text{H}_2\text{SO}_4$  film to equilibrate with  $\text{HCl}$  (or  $\text{HO}_2\text{NO}_2$ ) introduced from the gas phase and then measuring the  $\text{HO}_2\text{NO}_2$  (or  $\text{HCl}$ ) uptake. Partial pressures of PNA and  $\text{HCl}$  were maintained in the range of  $10^{-6}$  to  $10^{-7}$  Torr. For acid contents of 50 to 70 wt % and temperatures of 201 to 222 K, we observed no apparent reaction between PNA and  $\text{HCl}$ , nor any production of  $\text{Cl}_2$  or  $\text{HOCl}$ . (In the CIMS,  $\text{Cl}_2$  and  $\text{HOCl}$  can be detected using  $\text{SF}_6^-$  and  $\text{F}^-$  as  $\text{Cl}_2^-$  and  $\text{ClO}^-$ , respectively.) A conservative upper limit of  $10^4$  for this reaction was estimated based on our experimental conditions. Thus, we conclude that reaction 17 is of negligible stratospheric importance on sulfate aerosols.

#### *Stratospheric Implications*

Using the present determined effective Henry's solubility constants, equilibrium concentrations of PNA in sulfate aerosols can be estimated. For a nominal 55 wt %  $\text{H}_2\text{SO}_4$  aerosol at 205 K, the value for  $H^*$  is found to be  $2 \times 10^6 \text{ M atm}^{-1}$  according to Figure 8. This results in an equilibrium PNA concentration of about  $10^{-5} \text{ M}$  for a typical PNA mixing ratio of 0.1 ppbv at 100 mb (i.e. a partial pressure of  $10^{-8}$  Torr). At temperatures below 205 K, this equilibrium concentration should increase significantly, as indicated in Figure 8. Nevertheless, we believe that PNA is unlikely a major component of stratospheric aerosols, even when the

temperature is below 200 K, since PNA volatility is about two orders of magnitude smaller than that of  $\text{HNO}_3$  and the stratospheric PNA concentration is an order of magnitude smaller than that of  $\text{HNO}_3$ .

The distribution of PNA between the gas and condensed phases can be estimated by,

$$[\text{HO}_2\text{NO}_2(\text{aerosol})]/[\text{HO}_2\text{NO}_2(\text{g})] = P_{\text{PNA}} H^* L / (P_{\text{PNA}} / RT) = H^* L R T \quad (18)$$

where  $L$  is the volume fraction of the condensed phase in air. Using  $L$  values of  $10^{-14}$  and  $10^{-10}$  corresponding to 'background' and 'volcanically perturbed' aerosol conditions,<sup>36</sup> the ratios are about  $3.4 \times 10^{-7}$  and  $3.4 \times 10^{-3}$  at 205 K, respectively. In mid- or lower latitude stratosphere, where the ambient temperature is higher than 210 K, PNA should exist exclusively in the gas phase. Using an extrapolated value of  $6 \times 10^7 \text{ M atm}^{-1}$  for  $H^*$  at 195 K, this ratio can reach as high as 10 % for volcanic aerosol conditions. Hence, at conditions characteristic of polar stratosphere in the winter and of elevated sulfuric acid loading (such as that after the eruption of Mt. Pinatubo), incorporation of PNA into the sulfate aerosols may lead to a significant redistribution of PNA from the gas to condensed phase. This may affect stratospheric  $\text{NO}_x$  and  $\text{HO}_x$  concentrations, by reducing an important sink for OH radicals in the stratosphere (i.e. PNA reaction with OH).

Finally, the characteristic time required to reach equilibrium for the aerosol is estimated by,<sup>18</sup>

$$t = (2H^*RTd)/(3\alpha\omega) \quad (19)$$

Using a mean particle diameter of 0.1  $\mu\text{m}$  and an accommodation coefficient of 0.3, the characteristic time is about 0.04 s, suggesting that equilibrium between the gas and condensed phases is constantly maintained.

## Conclusions

In this paper we have reported laboratory measurements of interaction of PNA vapor with liquid sulfuric acid. PNA was observed to be physically taken up by sulfuric acid, without undergoing irreversible chemical reactions. The uptake data show that PNA is very soluble in liquid sulfuric acid: for a  $\text{H}_2\text{O}$  partial pressure of  $6.1 \times 10^4$  Torr the effective Henry's law coefficients were estimated to be in the range of  $1 \times 10^5$  to  $2 \times 10^6 \text{ M atm}^{-1}$  at temperatures between 205 and 220 K. In mid- or low latitude stratosphere, PNA should exist mainly in the gas phase.

At very colder stratospheric regions, uptake of PNA by sulfate aerosols may significantly reduce gaseous PNA concentration, thus affecting the  $\text{HO}_x$  and  $\text{NO}_x$  budgets. Heterogeneous reaction between PNA and HCl was concluded to be unimportant on sulfate aerosols in the stratosphere.

### **Acknowledgements**

The research was performed at the Jet Propulsion Laboratory, California Institute of Technology, under a contract with the National Aeronautics and Space Administration (NASA). We thank Z. Li, R.R. Friedl, and S.P. Sander for helpful discussions.



## References

- (1) DeMore, W.B.; Sander, S.P.; Howard, C.J.; Ravishankara, A. R.; Golden, D. M.; Kolb, C.E.; Hampson, R. F.; Kurylo, M. J.; Molina, M.J. *Chemical Kinetics and Photochemical Data for Use in Stratospheric Modeling*; JPL Publ. 94-26, NASA, 1994.
- (2) Kolb, C.E.; Worsnop, D.R.; Zahniser, M. S.; Davidovits, P.; Hanson, D.R.; Ravishankara, A.R.; Keyser, L.F.; Leu, M.T.; Williams, L.R.; Molina, M. J.; Tolbert, M.A. In *Current Problems in Atmospheric Chemistry*, J. R. Barker, Ed.; Adv. *Phys. Chem.*, World Scientific Publishing Company, Inc., 1995.
- (3) Turco, R.P.; Whitten, R.C.; Toon, O.B. *Rev. Geophys.* 1982,20,233.
- (4) Niki, H.; Maker, P. D.; Savage, C.M.; Breitenback, L.P. *Chem. Phys. Lett.* 1977,45,564.
- (5) Howard, C.J. *J. Phys. Chem.* 1977, 67, 5258.
- (6) Brasseur, G.; Solomon, S. *Aeronomy of the Middle Atmosphere*, D. Reidel Publishing Co.: Boston, 1984.
- (7) Yung, Y.L., private communication, 1995.
- (8) Macleod, H.; Smith, G. P.; Golden, D.M. *J. Geophys. Res.* 1988, 93, 3813.
- (9) Kenley, R. A.; Trevor, P. L.; Lan, B.Y. *J. Am. Chem. Soc.* **1981**,103, 2203.
- (10) Logager, T.; Sehested, K. *J. Phys. Chem.* 1993, 97, 10047.
- (11) Zhu, T.; Yarwood, G.; Chen, J.; Niki, H. *Environ. Sci. Technol.* **1993**, 27, 982.
- (12) Salawitch, R.J. et al. *Geophys. Res. Lett.* 1994, 23, 2551.
- (13) Wennberg, P.O. et al. *Science*, 1994, 266, 398.
- (14) Li, Z.; Friedl, R.R.; Sander, S.P. *J. Phys. Chem.*, submitted, 1995.
- (15) Baldwin, A. C.; Golden, D.M. *J. Geophys. Res.* **1980**, 85, 2888.
- (16) Zhang, R.; Leu, M.T.; Keyser, L. F., manuscript in preparation, 1995.
- (17) Danckwerts, P.V. *Gas-Liquid Reactions*; McGraw-Hill: New York, 1970.
- (18) Schwartz, S.E. In *Chemistry of Multiphase Atmospheric Systems*; Jaeschke, W., Ed.; NATO ASI Series, Vol. G6; NATO: Brussels, 1986.
- (19) Worsnop, D.R.; Zahniser, M. S.; Kolb, C. E.; Gardner, J. A.; Watson, L. R.; Van Doren, J.M.; Davidovits, P. *J. Phys. Chem.* 1989, 93, 1159.
- (20) Hanson, D. R.; Ravishankara, A.R. *J. Phys. Chem.* 1993, 97, 12309.

- (21) Brown, R. I. *J. Res. Natl. Bur. Stand. (U. S.)* 1978, 83, 1.
- (22) Marrero, T.R; Mason, E. A. *J. Phys. Chem. Ref. Data*, 1972, 1, 3.
- (23) Houghton, G. *J. Chem. Phys.* 1964, 40, 1628.
- (24) Luo, B.P.; Clegg, S. I.; Peter, T.; Muller, R.; Crutzen, P.J. *Geophys. Res. Lett.* 1994, 21, 49.
- (25) Williams, L. R.; Golden, D.M. *Geophys. Res. Lett.* 1993, 20, 2227.
- (26) Zhang, R.; Leu, M.T.; Keyser, L.F. *J. Phys. Chem.* 1994, 98, 13563.
- (27) Leu, M. T.; Tirnonen, R. S.; Keyser, L.F.; Yung, Y.L. *J. Phys. Chem.* submitted, 1995.
- (28) Zhang, R.; Leu, M.T.; Keyser, L.F. *J. Geophys. Res.*, in press, 1995.
- (29) Zeleznik, F.J. *J. Phys. Chem. Ref. Data* 1991, 20, 1157.
- (30) Zhang, R.; Wooldridge, P.J.; Abbatt, J.P.D.; Molina, M.J. *J. Phys. Chem.* 1993, 97, 7351.
- (31) Huey, L. G.; Hanson, D. R.; Howard, C.J. *J. Phys. Chem.*, submitted, 1995.
- (32) Sampoli, M.; De Santis, A.; Marziano, N. C.; Pinna, F.; Zingales, A. *J. Phys. Chem.* 1985, 89, 2864.
- (33) Zhang, R.; Wooldridge, P. J.; Molina, M.J. *J. Phys. Chem.* 1993, 97, 8541.
- (34) Leu, M.T.; Hatakeyama, S.; Hsu, K.J. *J. Phys. Chem.* 1989, 93, 5778.
- (35) Hanson, D. R.; Ravishankara, A.R. *J. Phys. Chem.* 1994, 98, 5728.
- (36) Hofmann, D.J.; Oltmans, S. J.; Solomon, S.; Deshler, T.; Johnson, B.J. *Nature*, 1992, 359, 183.

Table 1. Calculated Liquid-Phase Diffusion Coefficient  $D$ , (in units of  $10^{-8} \text{ cm}^2 \text{ S}^{-1}$ ) for PNA  
in Sulfuric Acid Based on the Cubic Cell Model

Temperature (K)	50 wt %	55wt%	60 wt %	65wt%	70wt%
210	3.1	2.2	1.4	0.8	0.3
220	8.0	6.1	4.2	2.6	1.3
230	17.2	13.6	10.0	6.6	3.8

Table 2. Measured Values of  $H^* \sqrt{D_l}$  for  $\text{HO}_2\text{NO}_2$  in Various  $\text{H}_2\text{SO}_4$  Solutions<sup>a</sup>

$P_{1120}$ (Torr)	$\text{H}_2\text{SO}_4$ wt % <sup>b</sup>	Temperature (K)	$H^* \sqrt{D_l}$ ( $\text{M atm}^{-1} \text{ cm s}^{-1/2}$ )
1.49X10 <sup>-3</sup>	52.9	208.9	169.9
		208.9	164.8
		214.4	<b>113.9</b>
		224.1	35.4
		229.1	22.0
6.86X10 <sup>-4</sup>	58.3	207.9	136.6
		207.9	<b>135.9</b>
		213.5	89.1
		<b>218.9</b>	48.1
		223.5	26.2
5.06x 10 <sup>-4</sup>	66.4	226.8	18.4
		201.4	88.6
		202.6	81.3
		205.4	57.8
		210.4	42.3
2.77x1 0 <sup>-4</sup>	73.8	215.1	27.0
		215.1	25.7
		204.1	2.67
		204.2	24.8
		208.0	19.7
		213.6	15.4
		219.0	11.1
		223.6	<b>8.8</b>
		223.6	9.1
		223.6	11.4

<sup>a</sup> Experimental conditions:  $P_{\text{He}} = 0.40$  Torr,  $V = 1700$  to  $2000 \text{ cm s}^{-1}$ , and  $P_{\text{PNA}} \approx 5 \times 10^{-7}$  Torr.

<sup>b</sup> Estimated from the temperature and water partial pressure.

Table 3. Measured Values of  $H^* \sqrt{D_l}$  for  $\text{HO}_2\text{NO}_2$  in  $\text{H}_2\text{SO}_4$   
at Different Temperatures<sup>a</sup>

Temperature (K)	$\text{H}_2\text{SO}_4$ wt % <sup>b</sup>	$H^* \sqrt{D_l} \pm 1\sigma$ ( $\text{M atm}^{-1} \text{cm s}^{-1/2}$ )
205.0	55.9	210.0 $\pm$ 14.5
210.7	61.7	62.4 $\pm$ 1.9
213.0	63.8	40.1 $\pm$ 1.2
216.6	66.5	24.0 $\pm$ 1.5
216.9	66.7	23.2 $\pm$ 1.3
218.0	66.9	21.5 $\pm$ 0.3
221.8	69.8	16.9 $\pm$ 1.1

<sup>a</sup> The experiments were performed by maintaining a constant water partial pressure at  $6.1 \times 10^{-4}$  Torr and by regulating temperature between 205 and 222 K. Each point is an average of more than two measurements. Experimental conditions are:  $P_{\text{He}} = 0.40$  Torr,  $V = 1700$  to  $2000 \text{ cm}^3 \text{ s}^{-1}$ , and  $P_{\text{PNA}} \approx 5 \times 10^{-7}$  Torr.

<sup>b</sup> Estimated from the temperature and water partial pressure.

## Figure Captions

- Figure 1. Mass spectrum of  $\text{SF}_6^-$  reaction with the effluent from a PNA bubbler.  $\text{F}^\bullet$  (HOZNOZ ( $m/e = 97$ )) is formed via a fluoride ion transfer from  $\text{SF}_6^-$  to  $\text{HO}_2\text{NO}_2$ . Impurities in the PNA sample are recognized primarily as  $\text{NO}_2$  ( $\text{NO}_2^-$ ,  $m/e = 46$ ) and  $\text{HNO}_3$  ( $\text{F}^\bullet \cdot \text{HNO}_3$ ,  $m/e = 82$ ). Other small, yet distinguishable peaks are due to  $\text{F}^\bullet$  ( $m/e = 19$ ),  $\text{NO}_3^-$  ( $m/e = 62$ ), and  $\text{SF}_4^-$  ( $m/e = 108$ ).
- Figure 2. Mass spectrum of  $\text{I}^-$  reaction with the effluent from PNA bubbler,
- Figure 3. Temporal profiles of PNA when exposed to a 3.9-cm length of sulfuric acid film at (a) 207.9 K, (b) 218.9 K, and (c) 226.8 K. The acid content of the film was estimated to be  $\sim 58.3$  wt %. Experimental conditions are:  $P_{\text{He}} = 0.40$  Torr,  $V \approx 1900$  cm S-I, and  $P_{\text{PNA}} \approx 5 \times 10^{-7}$  Torr.
- Figure 4. Uptake coefficients of PNA on liquid sulfuric acid as a function of temperature at  $P_{\text{H}_2\text{O}} = 6.1 \times 10^{-4}$  Torr. The values were determined from the initial decays of PNA signal upon exposure to liquid  $\text{H}_2\text{SO}_4$ . The acid content (top axis) was estimated ranging from about 56 to 70 wt %, as the temperature was varied from 205 to 222 K. Each point in the figure is an average of more than two measurements. The error bars represent one standard deviation of each determination. Experimental conditions are:  $P_{\text{He}} = 0.40$  Torr,  $V = 1700$  to  $2000$  cm s $^{-1}$ , and  $P_{\text{PNA}} \approx 5 \times 10^{-7}$  Torr.
- Figure 5. Measured values of  $H^\bullet \sqrt{D_t}$  against the reciprocal of temperature for various  $\text{H}_2\text{SO}_4$  contents. The solid lines are linear fits through the data. The estimated acid contents are labeled in the figure. Experimental conditions are:  $P_{\text{He}} = 0.40$  Torr,  $V \approx 1700$  to  $2000$  cm s $^{-1}$ , and  $P_{\text{PNA}} \approx 5 \times 10^{-7}$  Torr.
- Figure 6. Measured values of  $H^\bullet \sqrt{D_t}$  as a function of temperature at  $P_{\text{H}_2\text{O}} = 6.1 \times 10^{-4}$  Torr. Each point in the figure is an average of more than two measurements. The solid line is a least squares fit through the data. The top axis labels the estimated  $\text{H}_2\text{SO}_4$  content based on the temperature and water partial pressure in the flow tube. Experimental conditions are:  $P_{\text{He}} = 0.40$  Torr,  $V = 1700$  to  $2000$  cm s $^{-1}$ , and  $P_{\text{PNA}}$

$\approx 5 \times 10^{-7} \text{ Torr.}$

Figure 7. Same as **Figure 5** except for  $H^*$  calculated by estimating the liquid-phase diffusion coefficient using the cubic cell model.

Figure 8. Same as Figure 6 except for  $H^*$  calculated by estimating the liquid-phase diffusion coefficient using the cubic cell model.

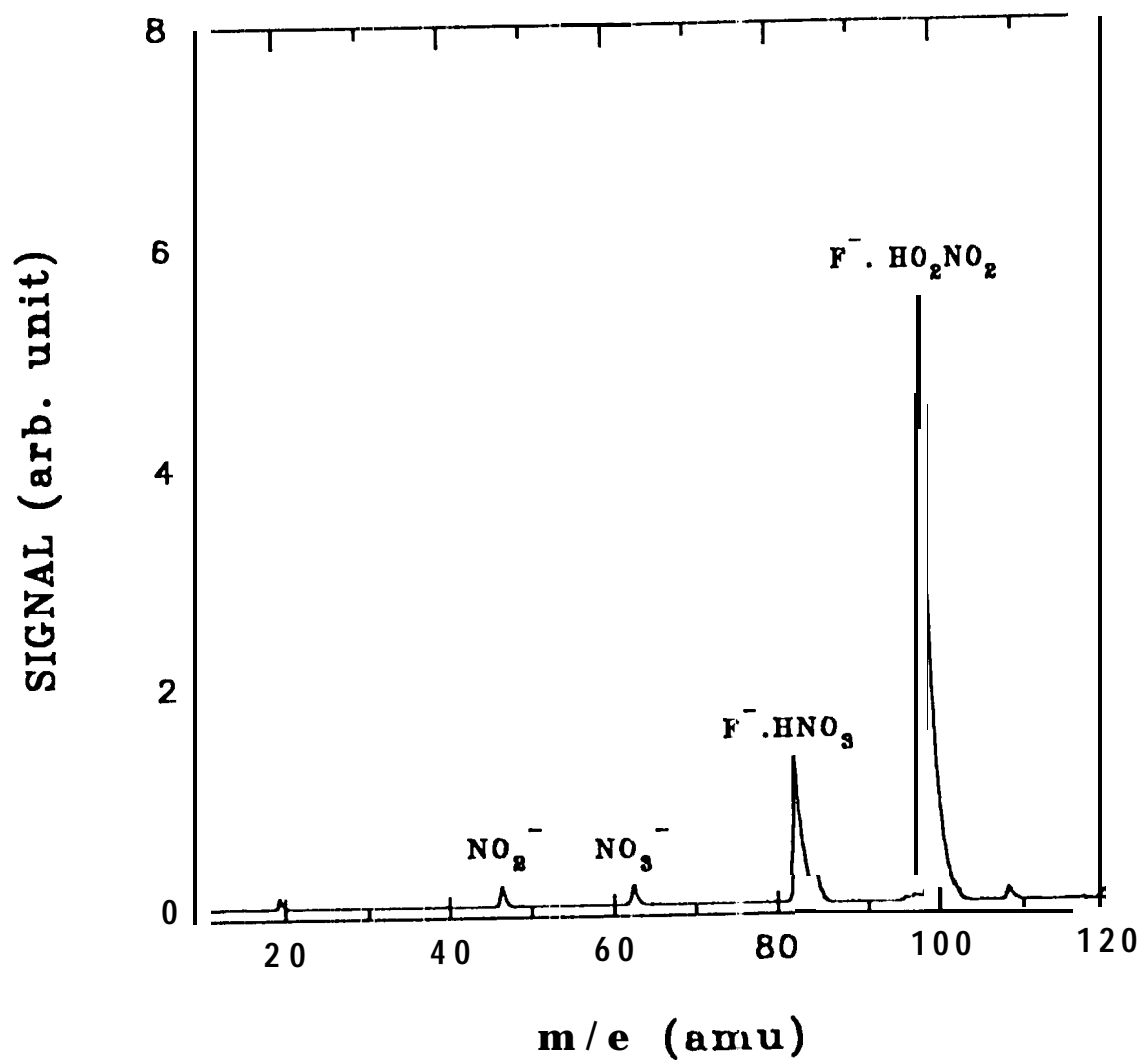
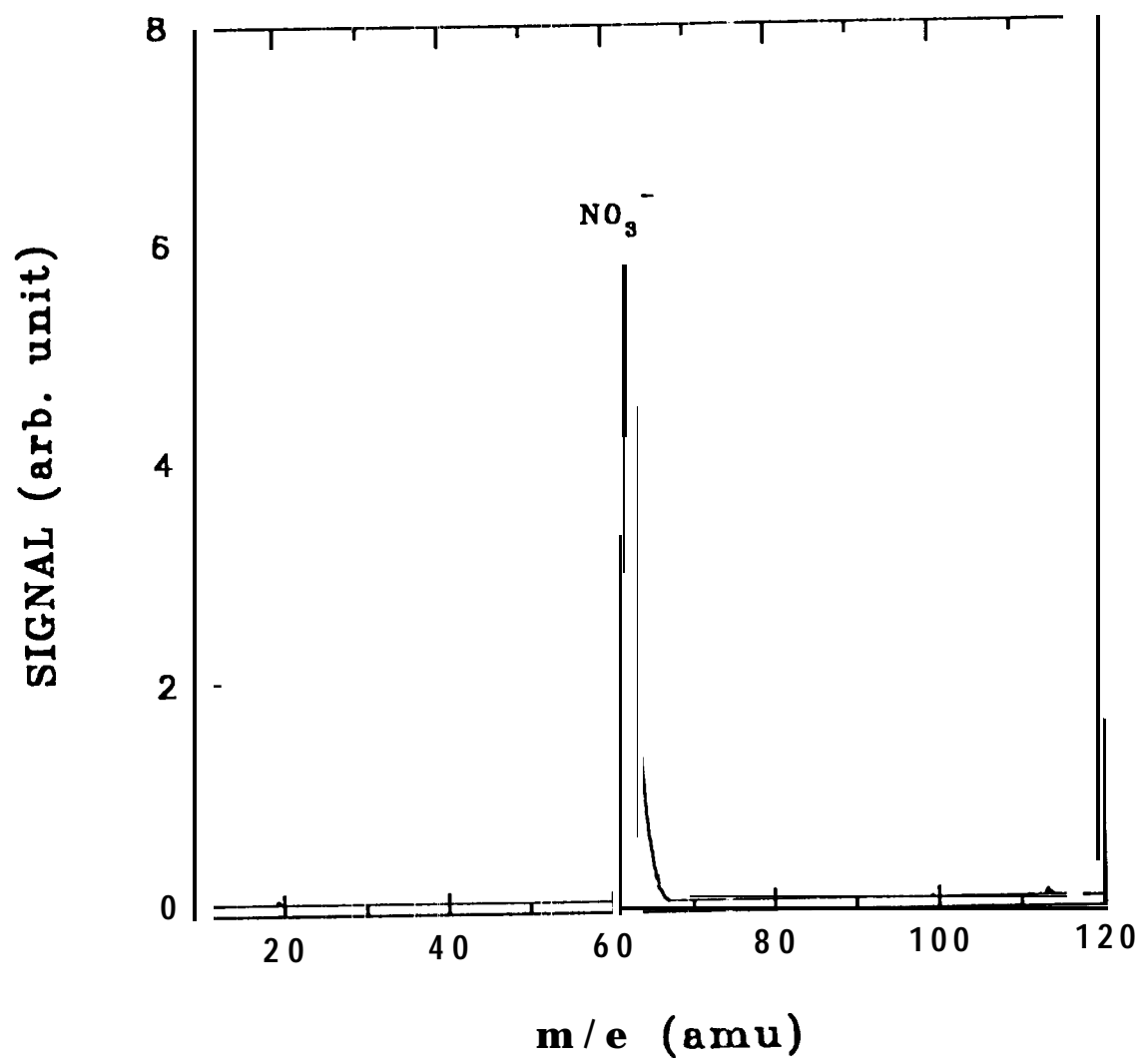


Fig. 1





SIGNAL (arb. units)

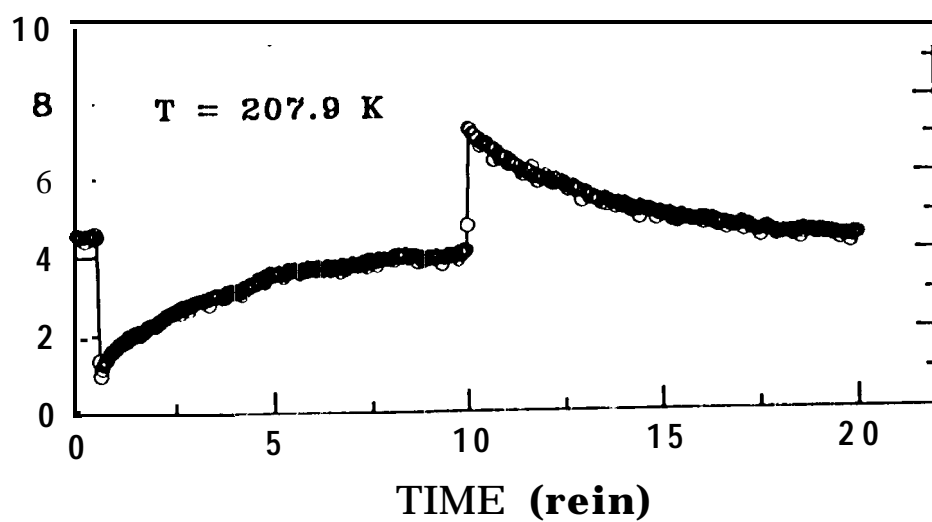
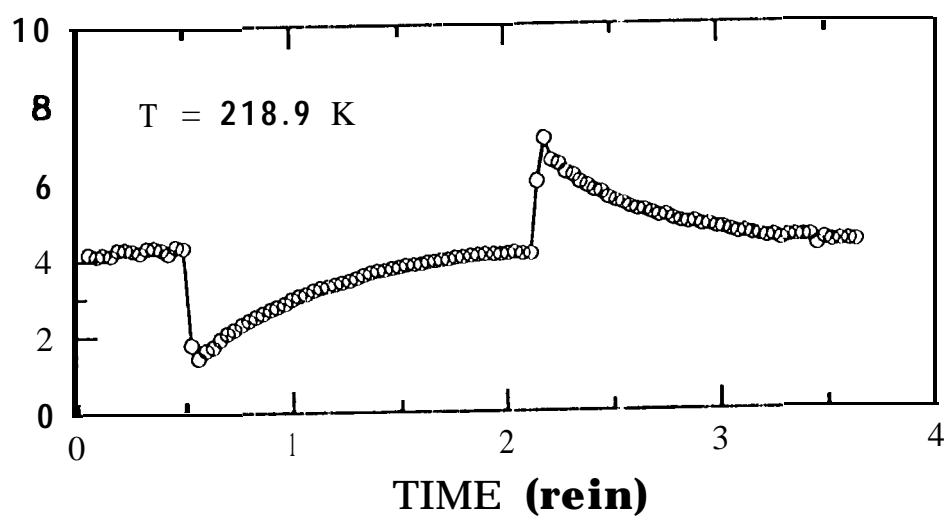
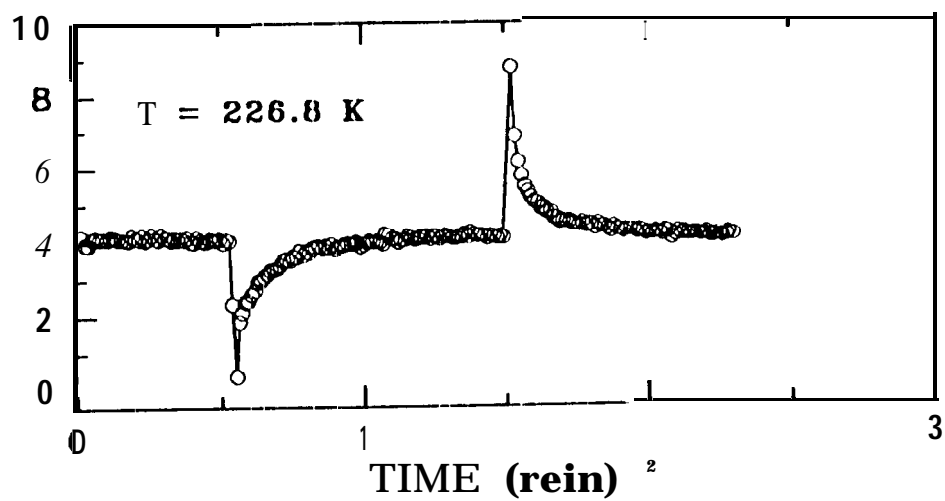


Fig. 3

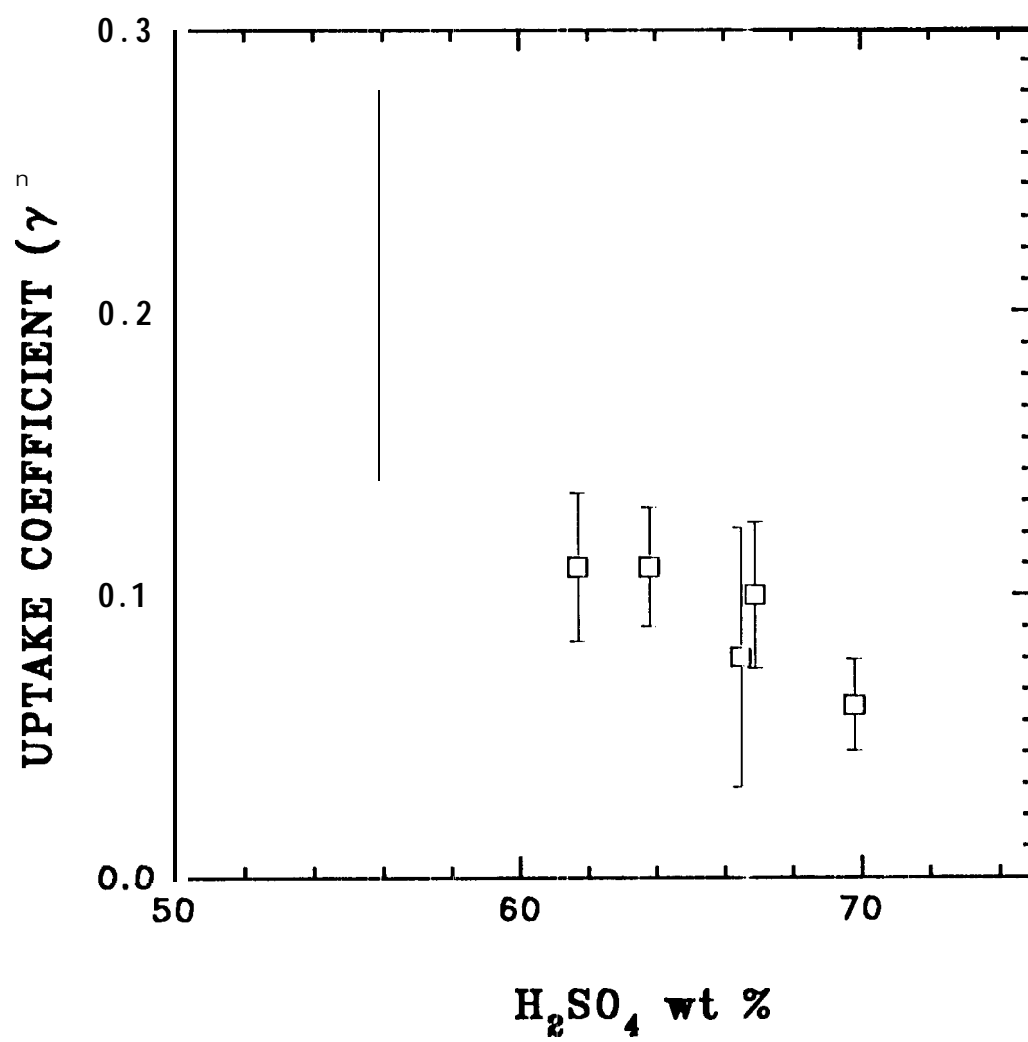


Fig 4

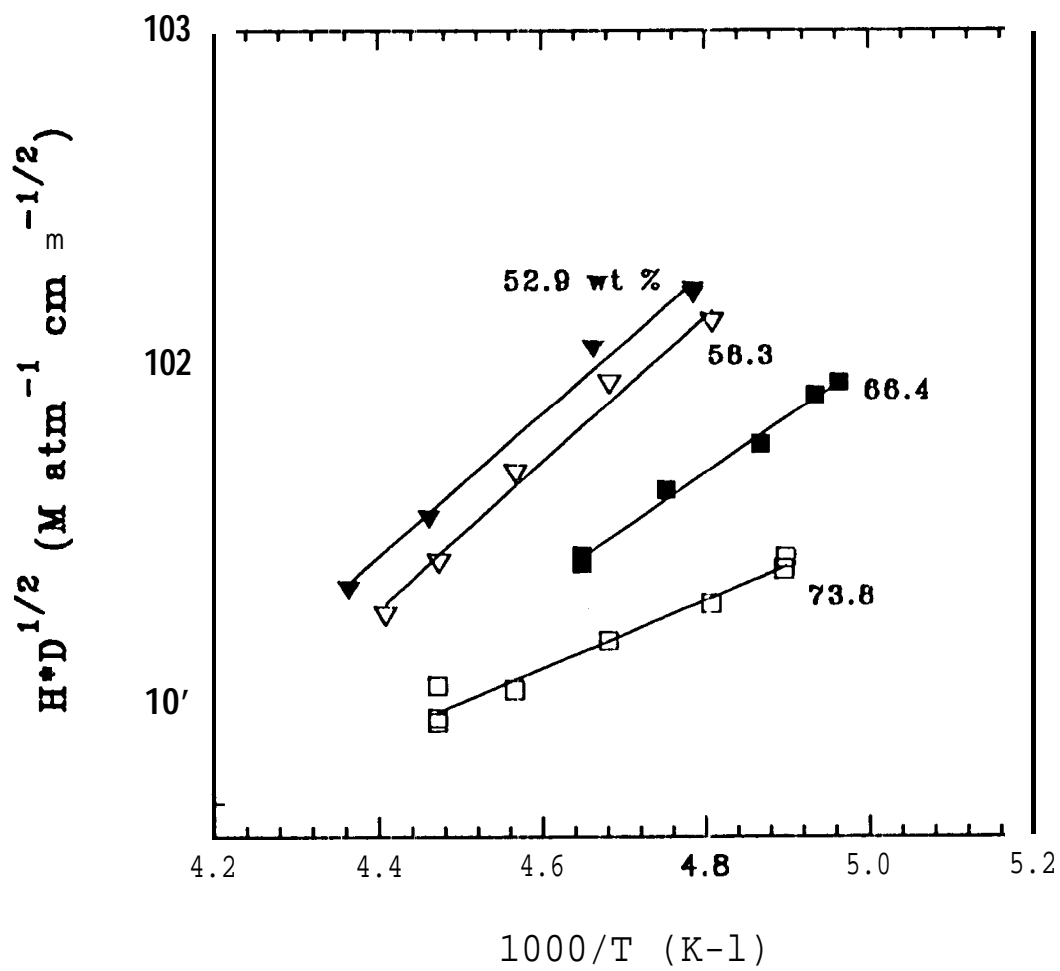


Fig. 5

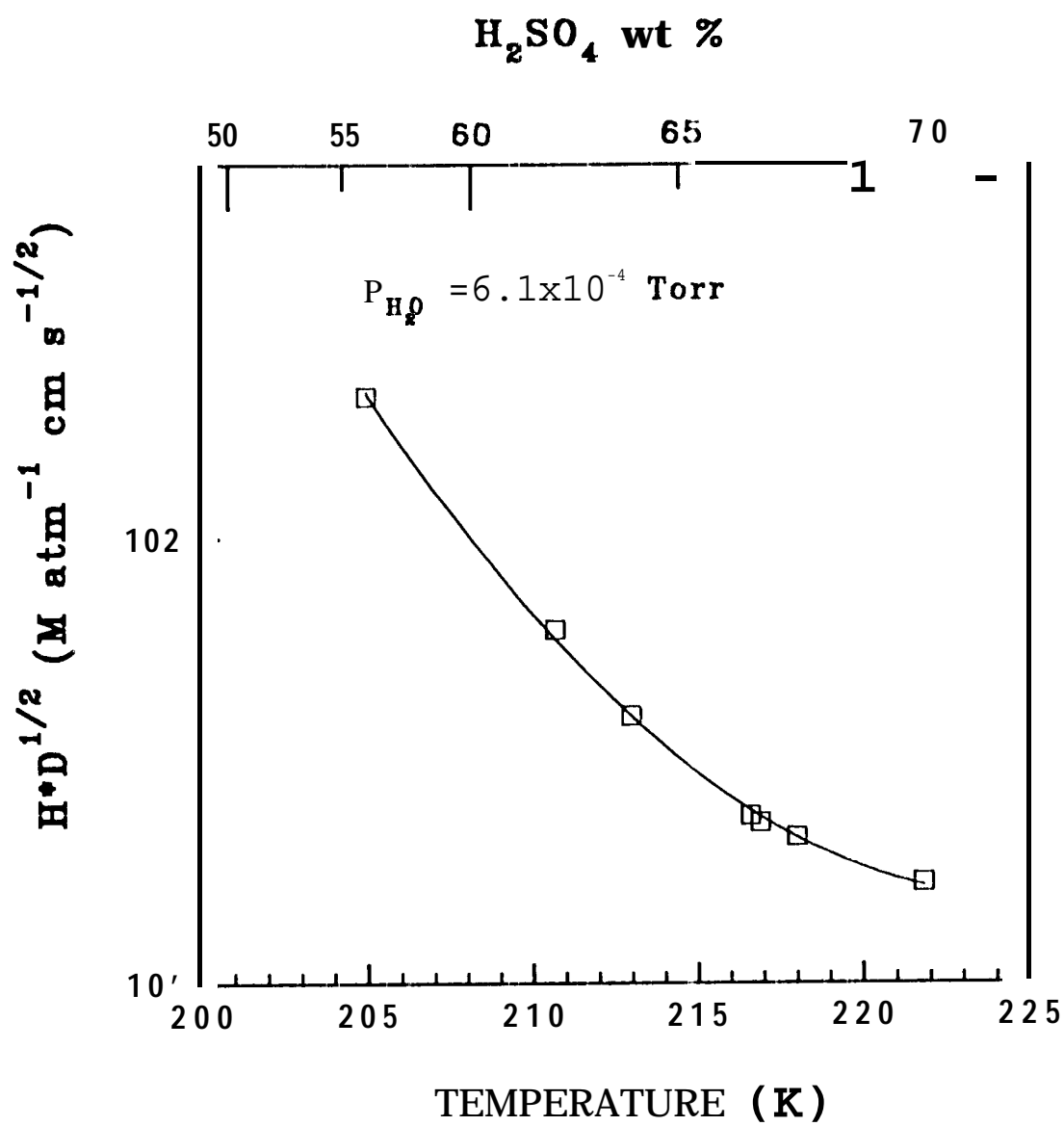
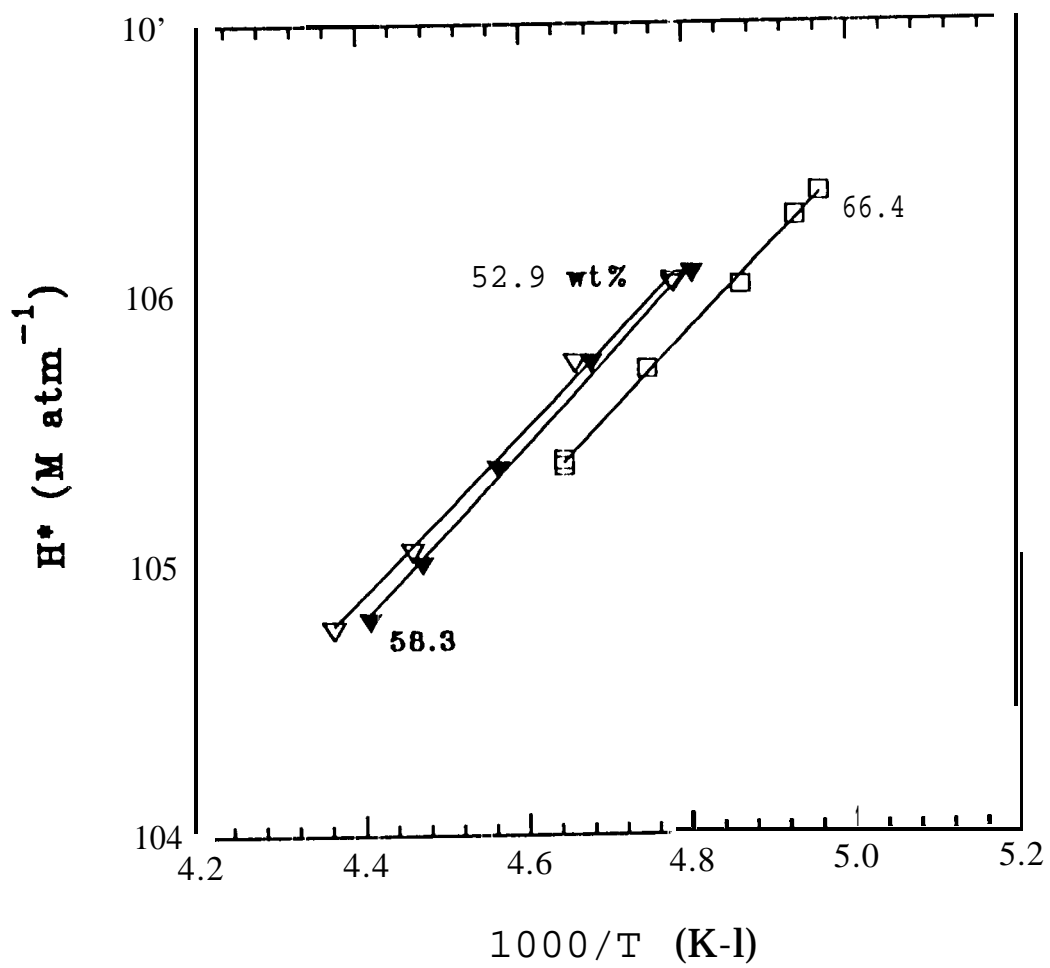


Fig. 6



F. 87

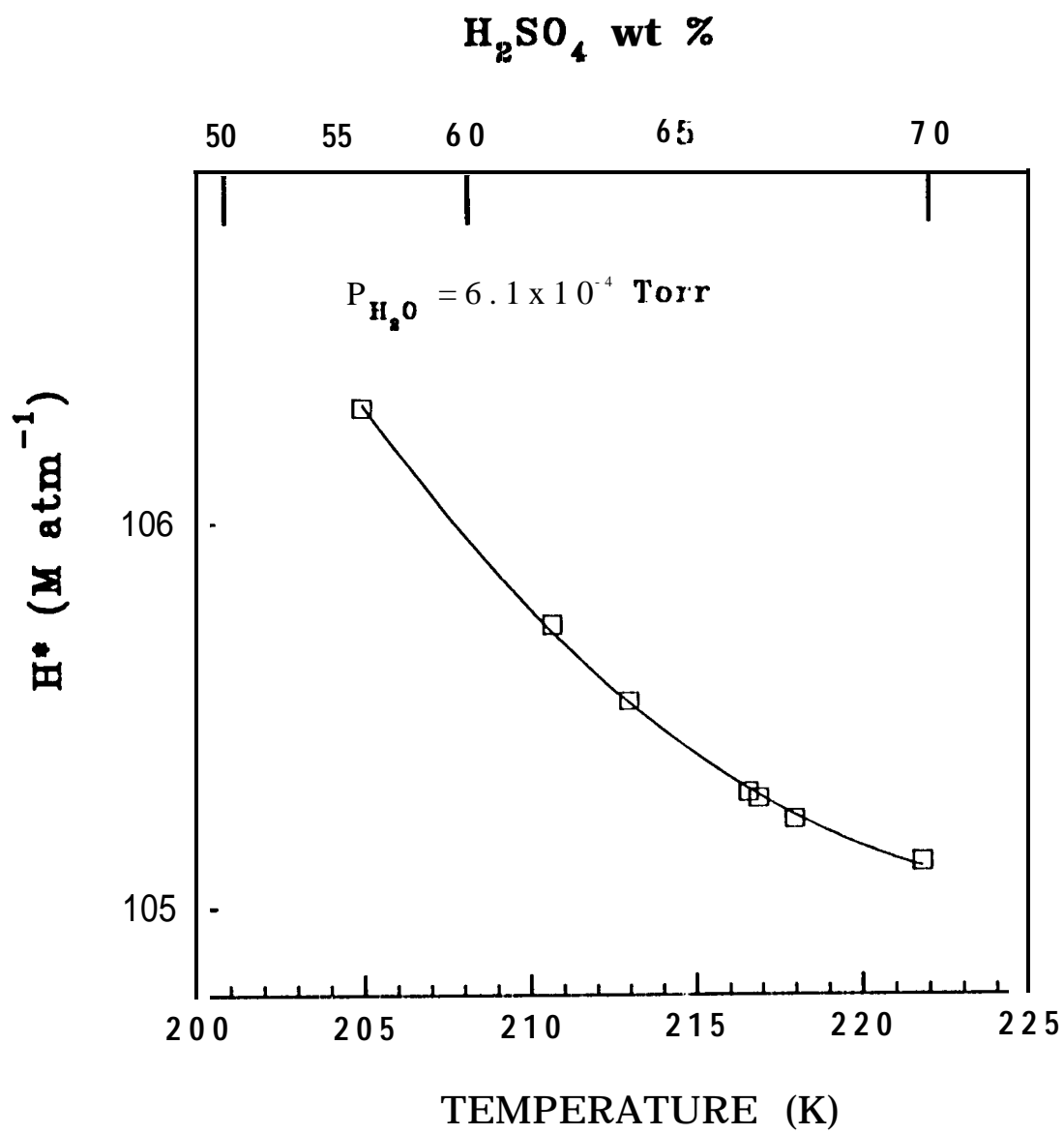


Fig. 2